C. R. Chimie 20 (2017) 1083–1092

Contents lists available at ScienceDirect

Comptes Rendus Chimie

www.sciencedirect.com

Full paper/Mémoire

Synthesis of a hierarchical ZSM-11/5 composite zeolite of high SiO_2/Al_2O_3 ratio and catalytic performance in the methanol-to-olefins reaction

Xiao Wang, Fanjun Meng, Hengbao Chen, Fei Gao, Yaquan Wang*, Xinpeng Han, Chunyang Fan, Chao Sun, Shuhai Wang, Li Wang

Key Laboratory for Green Chemical Technology of the Ministry of Education, School of Chemical Engineering and Technology, Tianjin University, Tianjin 300072, PR China

ARTICLE INFO

Article history:
Received 17 June 2017
Accepted 16 October 2017
Available online 16 November 2017

Keywords:
ZSM-11
CTAB
Seed
Template
Methanol to hydrocarbons

ABSTRACT

A hierarchical ZSM-11/5 composite zeolite with a high SiO_2/Al_2O_3 ratio was successfully synthesized using a seed-induced method in the presence of cetyltrimethylammonium bromide, characterized by scanning electron microscopy, X-ray diffraction, X-ray fluorescence, ^{27}Al NMR, ^{27}Si NMR, N_2 physical adsorption, and temperature-programmed desorption of ammonia, and studied in the frame of the methanol-to-olefins reaction. The results show that the amount of seed added plays a pivotal role in the formation of hierarchical ZSM-11/5 composite zeolite. With an increase in the amount of seed, the composite zeolite exhibits excellent catalytic performance in the methanol-to-olefins reaction, which can be attributed to the higher specific surface areas, higher external surface areas, more mesopore volumes, and more acid sites than ZSM-11 synthesized by the conventional method with tetrabutylammonium ions as a template. Contrary to the conventional point of view, the addition of too much seeds results in a dramatic decrease in the catalytic performance, which is ascribed to the higher proportion of ZSM-5 in the ZSM-11/5 composite zeolite.

© 2017 Académie des sciences. Published by Elsevier Masson SAS. All rights reserved.

1. Introduction

ZSM-11 is one type of high silica zeolite with MEL structure [1,2]. It has a three-dimensional topology composed of two perpendicularly intersecting straight channels along *a*- and *b*-axis. Its structure is closely related to that of ZSM-5, which has intersecting straight and sinusoidal channels [2]. This is the reason why ZSM-11 always forms composite with ZSM-5.

It has been found that many important reactions can be catalyzed by ZSM-11 or ZSM-11/5 composite zeolite. Varvarin et al. [3] reported that H-ZSM-5 and H-ZSM-11 showed similar conversion and yield in catalyzing the conversion of *n*-butanol to hydrocarbons. H-ZSM-11 also shows excellent catalytic properties in the conversion of low-density polyethylene to hydrocarbons [4], ethene to propene and butenes [5], methanol to olefins (MTOs) [6,7], methanol to propene [8], ethanol to propylene [9], and so forth. Directly synthesized Zn-ZSM-11 also shows excellent performance in catalyzing methanol to hydrocarbons [10] and superior catalytic properties to Zn-β zeolite in cracking of low-density polyethylene [11]. H-ZSM-11–supported Zn was also used to catalyze the activation of methane [12,13], the transformation of ethane into aromatic hydrocarbons [14], and so forth. Especially, ZSM-11 exhibits superior catalytic properties in some reactions to ZSM-5, such as higher paraffin hydroisomerization [15], dehydration of glycerol to acrolein

* Corresponding author.
E-mail address: yqwang@tju.edu.cn (Y. Wang).

https://doi.org/10.1016/j.crci.2017.10.004
1631-0748/© 2017 Académie des sciences. Published by Elsevier Masson SAS. All rights reserved.

[16], catalytic pyrolysis of heavy oil [17], conversion of methanol to light olefins [18] or hydrocarbons [19,20], aromatization and isomerization of 1-hexene [21], alkylation of benzene [22], ethanol conversion to light olefins and aromatics [23], and so forth.

ZSM-11 zeolite is commonly prepared by using tetrabutylammonium ions (TBA^+) as template (also called structure directing agent) ever since its discovery [3–5,11,14–48]. Fine ZSM-11 particles can be synthesized by low temperature crystallization [32]. Pure silica ZSM-11, silicalite-2 (S-2), can be synthesized from the clear gel solution with tetraethyl orthosilicate (TEOS) hydrolyzed in aqueous TBAOH [24,38]. However, in the absence of TBA^+, ZSM-11 cannot be synthesized with SiO_2 as silica source. Instead, pure magadiite was produced [37]. Of course, it has been found that the ZSM-11 zeolite synthesized with TBAOH as template is actually a ZSM-11/5 composite or intergrowth [25]. Pure phase ZSM-11 can be prepared with special templates such as 3,5-dimethylpiperidinium [49] and piperidine derivatives [50], 2,2-diethoxyethyltrimethylammonium [27,51], *N*,*N*-diethyl-3,5-dimethylpiperidinium hydroxide [27,52], and so forth. Jablonski and Sand [26] reported that to obtain a high content of ZSM-11 composite (>5% intergrowths), the synthesis should be carried out at low temperatures and with a high K/K + Na ratio [26]. Tsapatsis and co-workers [40,41] reported that the MFI–MEL intergrowth was an origin of orthogonal intergrowth leading to the formation of self-pillared hierarchical zeolite. Nevertheless, it is the ZSM-11 synthesized using TBAOH as template, that is, ZSM-11/5 intergrowth or composite that exhibits the above-mentioned superior catalytic properties in some reactions.

Although ZSM-11 zeolite shows excellent catalytic properties in many reactions, the narrow channels (0.53×0.54 nm) limit the accessibility of large molecules. Synthesis of zeolites with a hierarchical architecture of porosity is one of the most powerful methods to increase the accessibility of the internal surface area of zeolites because of the presence of mesopore and short diffusion path [53]. There have been several ways to introduce mesopores into the zeolitic crystals. To obtain hierarchical composite ZSM-11/5 zeolite, Song et al. [54] reported a solvent evaporation–induced self-assembly assisted by hexadecyltrimethoxysilane to produce a preformed dry gel, followed by its subsequent transformation into zeolite via steam-assisted crystallization. Chen et al. [55] used a diamine with linear carbon chains as a single template to obtain hierarchical ZSM-5 and ZSM-11 microspheres aggregated by nanocrystallines with mesopore after a long period (5–10 days) of crystallization at 448 K. When the carbon chains are C_8 and C_{10}, the product is ZSM-11. Yu et al. [17] synthesized hierarchical composite ZSM-11/5 zeolite using a small amount of TBABr combined with various crystallization modes. In this process, the small amount of TBABr was believed to direct the formation of both ZSM-11 framework and its intergrowth morphology, whereas the crystallization modes including one- and two-stage temperature-varying crystallization were mainly responsible for the adjustable particle size and mesoporous properties of the samples. With this method, hierarchical Zn-ZSM-11 can also be synthesized [56]. Xu and co-workers obtained hierarchical ZSM-11 zeolite by alkaline treatment with NaOH [57] or mixed solution of NaOH and cetyltrimethylammonium bromide (CTAB) [29]. Li et al. [22] also obtained mesoporous ZSM-5/11 composite zeolite bonded with alumina through alkaline treatment. Chen et al. [35] synthesized mesoporous ZSM-11 zeolite using binary templates of cetyltrimethylammonium tosylate and tetrabutylammonium hydroxide. Mesoporous ZSM-11 was also synthesized with TBA^+ as template and polyvinyl butyral [42] or carbon black [43,44] as mesopore generators.

In synthesizing zeolites with templates, after the synthesis, the templates must be removed through combustion, which releases a large amount of NO_x-containing gases. So, a great effect has been made to synthesize zeolites using seed-induced methods [58]. Seeds have been added to accelerate the crystallization rate of ZSM-11 [30]. Micron ZSM-11 microspheres were used to assist seed-induced synthesis of hierarchical submicron ZSM-11 with intergrowth morphology [31]. However, in the absence of template, ZSM-11 cannot be synthesized. At least a small amount of TBABr is necessary which was believed to direct the formation of both ZSM-11 framework and its intergrowth morphology [17]. In fact, it was reported that in the absence of template, ZSM-11 seeds resulted in the formation of ZSM-5 [59].

Our previous results showed that with ZSM-11 as seed in the absence of template TBA^+ ions or other specific templates, ZSM-5 was formed. However, by the addition of CTAB, ZSM-11/5 composite zeolite can be synthesized. The ZSM-11/5 composite zeolite with a SiO_2/Al_2O_3 ratio of 50 possesses hierarchical pores and shows excellent catalytic properties in the reaction of methanol conversion to gasoline [60].

Generally speaking, with seed-induced methods for the synthesis of zeolites, the higher the amount of the seed is added, the easier for the zeolites to form. However, when we used the seed-induced method for the synthesis of ZSM-11/5 composite with a high SiO_2/Al_2O_3 ratio, the results were not straightforward. In this article, we report that in synthesizing ZSM-11/5 composite zeolite with a high SiO_2/Al_2O_3 ratio of 170 in the absence of TBA^+, the amount of ZSM-11 added plays a pivotal role in the formation of ZSM-11/5 with hierarchical pores and the composite zeolite exhibits excellent catalytic performance in the MTO reaction, which is a potential route to replace petroleum with coal for the production of olefins [61–63].

2. Experimental section

2.1. Materials

Sodium aluminate ($NaAlO_2$, Analytical reagent (AR)), CTAB (AR), sodium hydroxide (NaOH, AR), and methanol (AR) were purchased from Tianjin Guangfu Fine Chemical Research Institute Co., Ltd. TEOS of 99 wt % was purchased from Tianjin Kemiou Chemical Reagent Co., Ltd. TBAOH (35 wt % in water) was purchased from Shanghai Cairui Chemical Co., Ltd. Silica sol (40 wt % suspension in water) was purchased from Qingdao Haiyang Chemical Co., Ltd.

Ammonium nitrate (NH_4NO_3, AR) was purchased from Guangdong Xilong Chemical Co., Ltd.

2.2. Synthesis of ZSM-11/5 composite zeolite with TBAOH as template

Silicalite-2 (S-2) was synthesized using a hydrothermal method according to Ref. [64–66]. ZSM-11/5 composite zeolite with a SiO_2/Al_2O_3 ratio of 170 was synthesized as follows: $NaAlO_2$ and NaOH were added to deionized water under vigorous stirring. After the solution became clear, tetrabutylammonium hydroxide was added. After the solution turned clear again, silica sol was added under vigorous stirring. Finally, S-2 was added. The gel molar composition was $8Na\text{-}100SiO_2\text{-}0.588Al_2O_3\text{-}2.5S\text{-}2\text{-}0.15TBAOH\text{-}2500H_2O$. The resulting slurry was left under stirring at room temperature for 4 h, and then transferred into a PTFE-lined autoclave, held first at 363 K for 24 h and then at 443 K for 48 h without stirring. After crystallization, the sample was cooled to room temperature and the precipitate was separated and washed with water until pH 7.5. The recovered solid was dried at 363 K for 12 h and then calcined at 823 K for 6 h in static air. To change the zeolite into H-form, the sample was stirred in 1 M solution of NH_4NO_3 (16.5 mL/g of solid) at 353 K for 2 h, then cooled, separated, and washed with deionized water through centrifugation until pH = 7.5. This ion exchange was repeated three times. The recovered sample was again dried at 363 K for 12 h and calcined at 823 K for 6 h in static air. The sample after calcination was denoted as SZ.

2.3. Synthesis of hierarchical ZSM-11/5 composite zeolites with a high SiO_2/Al_2O_3 ratio

Hierarchical ZSM-11/5 composite zeolites with a SiO_2/Al_2O_3 ratio of 170 were synthesized with addition of CTAB and calcined SZ as seeds in the absence of TBA ions. $NaAlO_2$ and NaOH were added to one-half of the deionized water required under vigorous stirring. After the solution became clear, SZ was added and then CTAB dissolved in another half of the deionized water was added. After the solution became clear again, silica sol was added dropwise under vigorous stirring. The final molar composition was $8Na\text{-}100SiO_2\text{-}0.588Al_2O_3\text{-}x\text{SZ-}2CTAB\text{-}2500H_2O$. The moles of SZ were calculated by combining both silicon and aluminum. The resulting slurry was left under stirring at room temperature for 4 h and then transferred into a PTFE-lined autoclave, held first at 363 K for 24 h and then at 443 K for 48 h without stirring. After crystallization, the autoclave was cooled to room temperature and the precipitate was separated and washed with water until pH = 7.5. The recovered solid was dried at 363 K for 12 h and then calcined at 823 K for 6 h in static air. The samples were also ion-exchanged, dried, and calcined as for SZ and are denoted as ZSM11-*x*SZ-2C, where *x* is the molar percentage of SZ relative to SiO_2.

2.4. Characterization

X-ray diffraction (XRD) patterns were obtained at room temperature using a Rigaku D/max2500 diffractometer employing the graphite filtered Cu Kα radiation ($\lambda = 0.1542$ nm) with a scanning rate of 8° min^{-1} in the 2θ ranges from 5° to 55°. The relative crystallinities were calculated by comparing the combination of the intensities of the four strong reflection peaks at 2θ of 7.92°, 8.78°, 23.14°, and 23.98°and taking that of SZ as 100%.

Secondary electron images (scanning electron microscopy [SEM]) were recorded using an S-4800 field emission scanning electron microscope of Hitachi with an accelerating voltage of 15 kV.

Solid-state magic angle spinning nuclear magnetic resonance (MAS NMR) was performed on a Varian infinity plus 300 MHz NMR spectrometer equipped at a field strength of 7.0 T. ^{27}Al MAS NMR spectra were recorded at 78.134 MHz at a spinning frequency of 8 kHz and 3 s intervals between successive accumulations. ^{29}Si MAS NMR spectra were recorded at 59.565 MHz at a spinning frequency of 4 kHz and 25 s intervals between successive accumulations.

SiO_2/Al_2O_3 ratios were measured using a Bruker AXS S4 Pioneer X-ray fluorescence spectrometer.

Nitrogen adsorption and desorption isotherms of the samples were measured at liquid N_2 temperature (77 K) using a Micromeritics TriStar 3000 automated physisorption instrument. Before the measurements, all the samples were degassed at 573 K for 4 h. The total specific surface area (S_{BET}) was derived from the Brunauer–Emmett–Teller (BET) equation. The external surface area (S_{ext}) was derived using the *t*-plot method, and the micropore surface area (S_{micro}) was calculated by subtracting S_{ext} from S_{BET}. The total pore volume (V_{total}) was obtained from the absorption amounts calculated at $p/p_0 = 0.99$. The micropore volume (V_{micro}) was also derived using the *t*-plot method, and the mesopore volume (V_{meso}) was calculated by subtracting V_{micro} from V_{total}.

Temperature-programmed desorption of ammonia (NH_3-TPD) measurements were recorded using a TP-5076 chemical adsorption instrument from Tianjin Xianquan Co., Ltd. The samples were pretreated in helium with a flow rate of 30 cm^3/min at 773 K for 1 h, then cooled down to 373 K, and ammonia was introduced with helium as the carrier gas. After 10 min of adsorption, the flow was switched to helium again, and the sample was heated to 973 K at a rate of 10 K min^{-1}. The desorbed ammonia was monitored using a thermal conductivity detector. The accuracy of the ammonia desorption amount measurement was within 3%.

Carbon deposition after the reaction was evaluated by thermogravimetric analysis (TGA) using a Shimadzu TGA-50 apparatus. The temperature was first kept at 550 K until the weight became constant and then increased to 1023 K at a heating rate of 10 K min^{-1} in oxygen atmosphere. The accuracy of the deposited carbon amount measurement was within 2%.

2.5. ZSM-11/5 composite zeolite-catalyzed MTOs

The MTO reaction was tested in a continuous flow fixed-bed reactor at 743 K under atmospheric pressure. The zeolite was pressed under 10 metric tons of pressure, crashed, and sieved into mesh size of 20–40 and 0.5 g of it was mixed with equal weight and the same size of quartz

and loaded into the middle section of a quartz tubular reactor with 20 mm of internal diameter and total length of 400 mm. A thermocouple was positioned in the center of the catalyst bed to monitor the temperature. The catalyst was first activated at 743 K for 1 h under high purity N_2 at a flow rate of 60 mL min^{-1}, before the start of the MTO reaction. Then, a liquid solution of methanol in water (50 mol %) was fed with an HPLC micropump, which was vaporized together with a flow rate of 60 mL min^{-1} of high purity nitrogen controlled using a mass flow controller. To compare the catalysts quickly, the reaction was conducted at a high weight hourly space velocity (WHSV) of methanol of 8 h^{-1}. An online gas chromatograph (GC-SP-3420) equipped with a flame ionization detector and a 50 m capillary column (HP-PLOT-Q) was used to analyze the products. To avoid possible condensation of high boiling point hydrocarbons, the temperature of the effluent line was constantly maintained at 453 K. The reaction performance results, including methanol conversion and product selectivity, were subsequently calculated by Eqs. (1) and (2), respectively.

$$\text{Methanol conversion}\,(\%) = \frac{N^{i}_{MeOH} - \left(N^{o}_{MeOH} + 2N^{o}_{DME}\right)}{N^{i}_{MeOH}} \times 100 \quad (1)$$

$$\text{Selectivity}\,(\%) = \frac{x \times N^{i}_{C_xH_y}}{N^{i}_{MeOH} - \left(N^{o}_{MeOH} + 2N^{o}_{DME}\right)} \times 100 \quad (2)$$

where N is the number of moles, superscripts i and o are the components at the inlet and outlet of the reactor, respectively, and x is the number of carbon atoms. DME (dimethyl ether) was considered as a reactant.

3. Results and discussion

3.1. Characterization

Fig. 1 shows the XRD patterns of SZ and the samples synthesized by the addition of SZ as seed in the presence of CTAB. The XRD pattern of SZ prepared with TBAOH as template exhibits the characteristic diffraction peaks of ZSM-11 at $2\theta = 7.92°$, 8.78°, 23.14°, and 23.98°, without strong reflections at 2θ of 23.38°, 23.82°, and 24.47° [17,19,42,43], confirming that the seed is ZSM-11. Addition of SZ at a seed/SiO_2 molar ratio of 1, the intensity of the sample is very low. With an increase in the amount of seed added, the relative crystallinities increase. The reflections at 2θ of 23.38° and 23.82° are nearly indiscernible and only the one at 24.47° is apparent, indicating that the zeolite contains limited amount of the ZSM-5 phase. Nevertheless, the zeolite is called ZSM-11/5 composite. However, when the amount of seed added is up to the seed/SiO_2 molar ratio of 6, the shoulders at the higher angle side of the peak of $2\theta = 23.14°$ and the lower angle side of the peak of $2\theta = 23.98°$ split apparently, indicating that the proportion of ZSM-5 is appreciable.

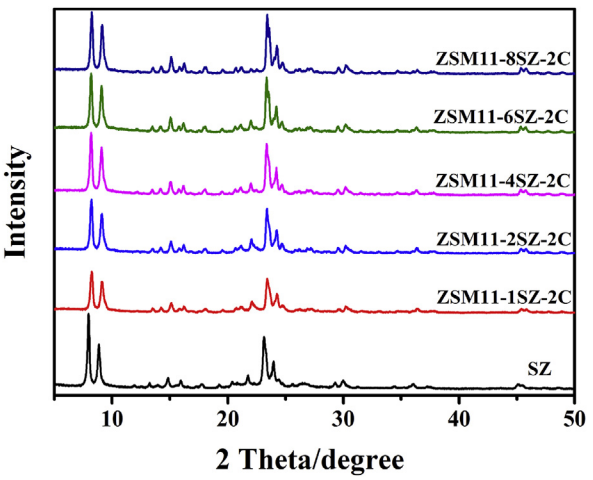

Fig. 1. XRD patterns of samples synthesized with different amounts of SZ as seed.

Generally speaking, with the seed-induced method for the synthesis of zeolites, the more the amount of the seed is added, the easier for the zeolites to form. However, for the synthesis of ZSM-11/5 composite with a high SiO_2/Al_2O_3 ratio (170), the present results demonstrate that the amount of ZSM-11 seed added plays a pivotal role in the formation of the ZSM-11/5 composite zeolite, with too much seed resulting in the formation of high proportion of ZSM-5 in the composite.

In the absence of CTAB, SZ itself causes the formation of pure ZSM-5 at much lower temperature than that required for the formation of ZSM-11 [60]. It implies that ZSM-5 is much easier to form than ZSM-11. CTAB has the function of intercalation. The head groups of CTA^+ cations are anchored to the surface aluminosilicate by strong electrostatic interaction with uniform distribution [67]. The tail alkyl groups would prevent the other aluminosilicate ions approaching, deterring the formation of ZSM-5. So, the ZSM-11 seed has the chance to promote the formation of ZSM-11. When the amount of SZ is increased, the function of CTAB weakens and the growth rate of ZSM-5 increases. So, when the amount of seed added is up to the seed/SiO_2 molar ratio of 6 or above, higher proportion of ZSM-5 is formed in the composite. Addition of more CTAB does not work, probably because of its low solubility, especially in the presence of a large amount of inorganic materials, which further decreases its solubility.

Fig. 2 shows the SEM images of samples synthesized with the different amounts of seeds. SZ has small particle sizes of about 850 nm. The particle sizes of the samples synthesized with SZ and addition of CTAB are much larger than the seed SZ prepared with TBAOH as template. However, this does not mean that the crystallites of the samples are large. In fact, the particles are aggregates of small zeolite crystallites. With the addition of SZ at a low level (seed/SiO_2 molar ratio of 1), there are some amorphous materials, agreeing with the XRD results that the materials are not fully crystallized into the zeolite. This is the reason why the intensity of the sample is low. With an increase in the amount of seed, the sizes of the aggregates increase to some extent.

The SiO_2/Al_2O_3 ratios and the relative crystallinities are given in Table 1. The SiO_2/Al_2O_3 ratios are slightly lower than the nominal ones (170), but there are no much

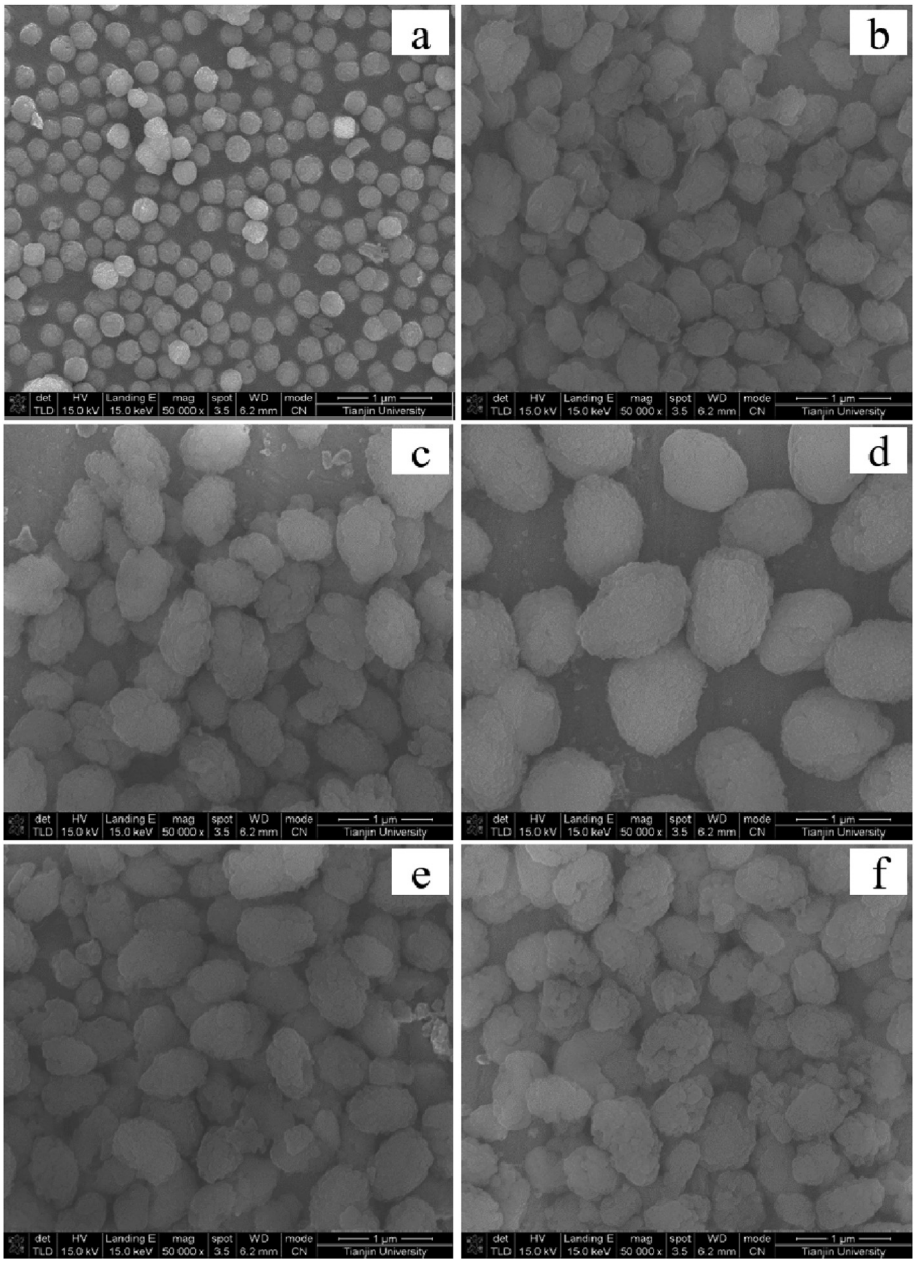

Fig. 2. SEM images of samples synthesized with different amounts of SZ as seed: (a) SZ; (b) ZSM11-1SZ-2C; (c) ZSM11-2SZ-2C; (d) ZSM11-4SZ-2C; (e) ZSM11-6SZ-2C; and (f) ZSM11-8SZ-2C.

differences among all the samples. The relative crystallinities of the ZSM-11/5 composite zeolites are lower than that of SZ, which is taken as 100%. The results demonstrate that although the aggregate sizes of the ZSM-11/5 composite zeolites are much larger than that of SZ, the primary crystals in these ZSM-11/5 composite zeolites may be much smaller and/or the aggregates may be more porous than those of SZ.

^{27}Al MAS NMR and ^{29}Si MAS NMR spectra are shown in Fig. 3. ^{27}Al MAS NMR spectrum can verify if the aluminum is incorporated in the zeolite framework. In general, the resonance centered at around 54 ppm is commonly assigned to four-coordinated framework aluminum, whereas the peak at 0 ppm refers to nonframework octahedral aluminum. There is no discernible peak at 0 ppm in any of the samples, implying that aluminum is in the framework of the zeolites, and no nonframework aluminum exists. The ^{29}Si MAS NMR spectra show clearly the Si(0Al) species and discernible Si(1Al) species. No Si(2Al) species are discernible because the SiO_2/Al_2O_3 ratio is high.

The N_2 adsorption–desorption isotherms of the synthesized ZSM-11/5 composite zeolites are shown in Fig. 4,

Table 1
Textural properties of ZSM-11/5 composite with different amounts of seed.

Sample	SiO_2/Al_2O_3 ratios	RC[a]	Surface area (m^2/g)			Pore volumes (cm^3/g)		
			S_{BET}	S_{Micro}	S_{Ext}	V_{Total}	V_{Micro}	V_{Meso}
ZSM11-8SZ-2C	162	93	371	239	132	0.196	0.108	0.088
ZSM11-6SZ-2C	165	87	385	229	156	0.236	0.126	0.110
ZSM11-4SZ-2C	167	85	397	234	163	0.251	0.130	0.121
ZSM11-2SZ-2C	164	76	373	235	138	0.233	0.116	0.117
ZSM11-1SZ-2C	162	71	347	215	132	0.187	0.099	0.088
SZ	164	100	211	165	46	0.191	0.122	0.069

[a] Relative crystallinity.

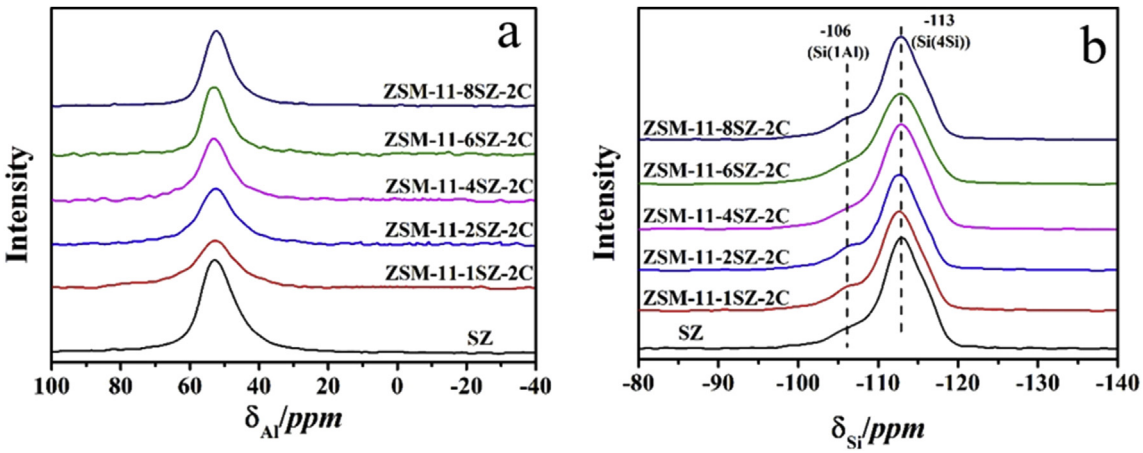

Fig. 3. ^{27}Al MAS NMR (a) and ^{29}Si MAS NMR (b) spectra of samples synthesized with different amounts of SZ as seed.

and the textural properties of these samples are summarized in Table 1. SZ exhibits type I isotherm according to the IUPAC classifications, indicating that the composite zeolite is absolutely microporous. For those samples synthesized in the presence of CTAB, with the addition of SZ as seed, the adsorption and desorption isotherms exhibit hysteresis loops, which are hybrid of types I and IV, indicating that the samples also contain mesopores. So, the ZSM-11/5 composite zeolites should be called hierarchical ZSM-11/5 composite zeolites. The horizontal hysteresis loop could relate to some secondary porosity that is in contact with the exterior though channels of zeolite. With the addition of more SZ, the loops become larger.

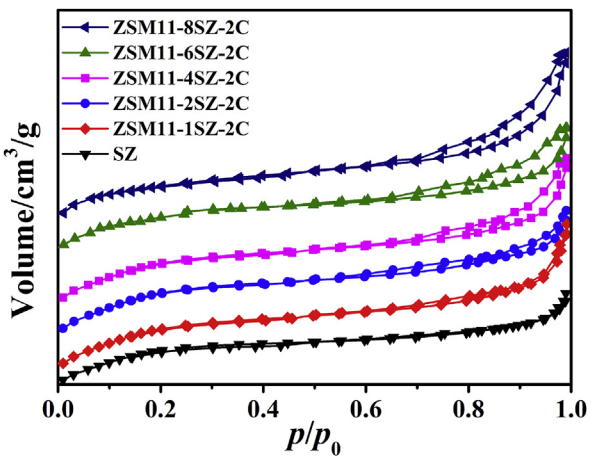

Fig. 4. N_2 adsorption–desorption isotherms of samples synthesized using different amounts of SZ as seed.

Because the head groups of CTA^+ cations are anchored to the aluminosilicate surface by strong electrostatic interaction [67], they would also prevent further condensation of the same crystals and finally lead to the formation of aggregates of ZSM-11/5 composite zeolite with hierarchical pores. Garcia-Martinez et al. [68,69] successfully introduced controlled mesoporosity into zeolite crystals using a surfactant templating approach. The zeolites were treated with a CTAB solution in NH_4OH (or other bases such as NaOH, Na_2CO_3, and so on) to introduce mesoporosity. A crystal rearrangement mechanism for the mesopore formation was proposed: the mesopores form when the surfactant molecules self-assemble inside the framework structure and the crystal structure rearranges to accommodate them. Although CTAB was added in the gel for the synthesis of the ZSM-11/5 composite zeolite in this work, rather than post-treatment with CTAB solution in alkaline, the presence of both CTAB and alkaline may also cause the formation of mesopores to some extent through the crystal rearrangement mechanism.

The specific surface areas, external surface areas, total pore volumes, and mesopore volumes also increase with the addition of SZ above the seed/SiO_2 molar ratio of 1 and reach to the highest values at the seed/SiO_2 molar ratio of 4.

This obviously can be attributed to the hierarchical pores caused by the addition of CTAB. This may also be one reason why the aggregates with large particle sizes have lower intensity in the XRD reflections. The results also imply that these ZSM-11/5 composite zeolites may be good catalysts for some reactions because more acid sites could be accessible by large molecules and the mesopores can accommodate more deposited carbons. With further increase in the amount of SZ, the specific surface areas, external surface areas, total pore volumes, and mesopore volumes decrease to some extent. This can be ascribed to the increase in the proportion of ZSM-5 in the ZSM-11/5 composite.

Fig. 5 shows the NH_3-TPD profiles of the ZSM-11/5 composite zeolites. The acid densities derived from the NH_3-TPD profiles are tabulated in Table 2. There are two desorption peaks in NH_3-TPD curves for each sample. The low temperature peaks and the high temperature peaks are attributed to weak and strong acid sites, respectively. The peak temperatures of both the low and the high temperature peaks are very close on each sample. The results demonstrate that the ZSM-11/5 composite zeolites with hierarchical pores by our method do not alter the acidic strength of both the weak and strong acids. This is understandable because the acid strength of structurally similar aluminosilicate-type zeolites mainly depends on the framework SiO_2/Al_2O_3 ratios [6], not to mention for the same zeolite, and the SiO_2/Al_2O_3 ratios of all the zeolites including the seed SZ are almost the same. However, with increase in the amount of SZ, both the weak and strong acid densities as well as the total acid densities all increase markedly. Obviously, the results arise from the mesopore formation and the acid densities increase with the specific surface areas. It seems that the total acid densities, the weak acid densities, and the strong acid densities all increase in proportion. Again, this is understandable because the SiO_2/Al_2O_3 ratios of all the zeolites are almost the same. However, when the amount of seed added is up to the seed/SiO_2 molar ratio of 6 or above, the total acid densities, the weak acid densities, and the strong acid densities all decrease to some extent. Liu et al. [23] reported that ZSM-11 zeolite exhibits lower acid density compared to ZSM-5 with the same SiO_2/Al_2O_3 ratio. With the increase in SiO_2/Al_2O_3 ratios, the acid densities should decrease because they come from the aluminum in the zeolite framework. However, Zhang et al. [21] reported that ZSM-11 with the SiO_2/Al_2O_3 ratio of 80 exhibits even more acid densities than ZSM-5 with the SiO_2/Al_2O_3 ratio of 50. Considering that very similar structure between ZSM-5 and ZSM-11, if the SiO_2/Al_2O_3 ratios are the same, the number of the acid densities should be related to the specific surface area. When the amount of seed added is up to the seed/SiO_2 molar ratio of 6 or above, the proportion of ZSM-5 in the composite increases, whereas the specific surface area decreases. This might be the reason why the total acid densities, the weak acid densities, and the strong acid densities all decrease to some extent.

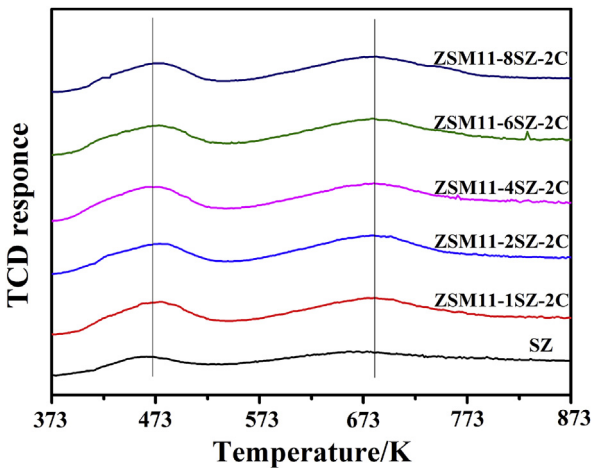

Fig. 5. NH_3-TPD of samples synthesized with different amounts of SZ as seed.

Table 2
Acid amounts of ZSM-11/5 composite with different amounts of seed.

Samples	Acid amounts (mmol/g)[a]		
	Total acidity	Weak acidity	Strong acidity
ZSM11-8SZ-2C	0.299	0.120	0.179
ZSM11-6SZ-2C	0.326	0.134	0.192
ZSM11-4SZ-2C	0.368	0.157	0.211
ZSM11-2SZ-2C	0.319	0.135	0.184
ZSM11-1SZ-2C	0.315	0.144	0.171
SZ	0.211	0.086	0.125

[a] Calculated by NH_3-TPD.

3.2. ZSM-11/5 composite zeolite-catalyzed MTOs

Fig. 6 shows the changes of methanol conversions and selectivities of olefins in the MTO reaction with reaction time catalyzed by samples synthesized with different amounts of seed. There are no appreciable differences in the selectivity of the olefins among all the catalysts, around 37% selectivity of propene and 70% selectivity of C_2–C_4 olefins. ZSM11-4SZ-2C has a slightly higher selectivity of C_2–C_4 olefins. This obviously can be attributed to the same acidic strength, further to the same SiO_2/Al_2O_3 ratio, and to the proportional increase in the total acid densities, the weak acid densities, and the strong acid densities of the hierarchical ZSM-11/5 composite zeolites compared with SZ.

Methanol conversions and hydrocarbon distributions of samples synthesized with different amounts of seed in methanol to olefins reaction are given in Table 3. The selectivities to C_{1-4} alkanes on the hierarchical ZSM-11/5 composite zeolites (6.9–8.4%) are higher than those of SZ (4.2%). It is well known that shorter diffusional paths, for example, small particle sizes of the zeolites or more accessible domains of zeolites decrease the probability of saturation of olefins via hydride transfer reactions, eventually helping to increase light olefins yields [70]. The V_{Micro}/V_{Meso} ratio of SZ is about 2, about two times of those of the hierarchical ZSM-11/5 composite zeolites. Presumably, the selectivities of C_{1-4} alkanes on SZ should be higher than those on the hierarchical ZSM-11/5 composite zeolites. However, the selectivities of aromatics on SZ are also

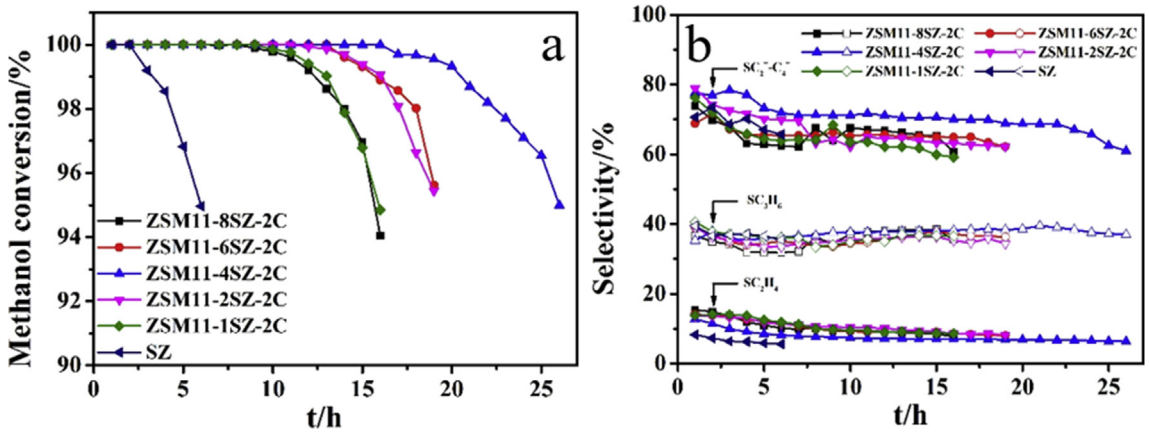

Fig. 6. Changes in methanol conversions and selectivities of olefins in the MTO reaction with reaction time catalyzed by samples synthesized with different amounts of SZ as seed. (a) Methanol conversions and (b) selectivities of olefins.

higher. On one hand, ZSM-11 is a good catalyst for aromatization, which converts alkanes into aromatics [12–14]. On the other hand, after 3 h online, SZ deactivates to some extent. The conversion of methanol is 99.2%, while the hierarchical ZSM-11/5 composite zeolites have not deactivated. The deposited carbon may prevent the hydride transfer reactions, and therefore leads to the lower selectivities of $C_{1\text{-}4}$ alkanes on SZ.

The initial methanol conversions of all the samples under the present conditions are 100%. With the reaction proceeds online, the methanol conversions gradually decrease. For the catalyst stability, there are much differences among the catalysts. Here, the catalyst life is defined as the time from the beginning of the reaction to the point when the methanol conversion just drops below 95%. SZ has a catalyst life of only 6.0 h. With an increase in the seed in the synthesis of the ZSM-11/5 composite zeolites, the catalyst life increases markedly, that is, from about 15.9 h on ZSM11-1SZ-2C to 19.2 h on ZSM11-2SZ-2C and to 26.1 h on ZSM11-4SZ-2C. It should be reiterated that to compare the zeolite catalysts quickly, the reactions were conducted at a high WHSV (8 h^{-1}) rather than below 1 h^{-1} used in industry. A few hours longer of the catalyst life in the testing means much longer of the operating time in the industrial reactor. Under the same conditions, a commercial ZSM-5 with the same SiO_2/Al_2O_3 ratio has the catalyst life of only 7.5 h [66]. However, with further increase in the amount of SZ in the synthesis, the catalyst life decreases, that is, to about 19.1 h on ZSM11-6SZ-2C and 15.6 h on ZSM11-8SZ-2C.

After the catalytic evaluations, the deactivated zeolites were further characterized by TGA and the results are given in Fig. 7. The mass losses of the catalysts in air flow over the temperature range of 470–950 K are related to combustion of the coke deposited on the deactivated zeolites. The coke contents occurred in the hierarchical ZSM-11/5 composite zeolites are higher than that in SZ because the former runs for longer time than the latter. However, if the coke contents are divided by the reaction time online, the carbon deposition rates, as shown in Fig. 8, on the hierarchical ZSM-11/5 composite zeolites, especially on ZSM11-4SZ-2C, are much lower than that on SZ.

In comparison with ZSM-5, ZSM-11 has not been studied much for the MTO reaction. In the few reports [6,7,18–20], the purposes for the end products were different with the zeolite of different SiO_2/Al_2O_3 ratios and different reaction conditions used, which make it difficult to compare with the present results. Dyballa et al. [6] investigated the MTO reaction on zeolites ZSM-5 and ZSM-11 and found that both

Table 3
Methanol conversions and hydrocarbon distributions of samples synthesized with different amounts of seed in the MTO reaction (Time on stream = 3 h, 743 K, 0.1 MPa, WHSV = 8 h^{-1}).

Samples	Methanol conversions (%)	Selectivity (%)				
		$C_{1\text{-}4}$	$C_2^=$	$C_3^=$	$C_4^=$	C_{5+}
ZSM11-8SZ-2C	100	8.4	13.8	34.2	19.8	23.8
ZSM11-6SZ-2C	100	8.0	13.6	34.7	20.8	22.9
ZSM11-4SZ-2C	100	6.9	9.9	35.9	21.4	25.9
ZSM11-2SZ-2C	100	7.0	13.3	35.4	21.3	23.0
ZSM11-1SZ-2C	100	6.9	14.1	37.1	20.1	21.8
SZ	99.2	4.2	6.4	36.7	25.6	27.1

C_{5+}: hydrocarbons with five or above carbons.

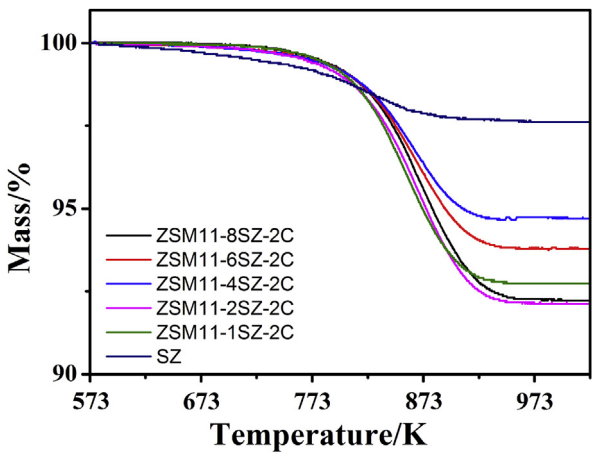

Fig. 7. TGA profiles of samples synthesized with different amounts of SZ as seed after the MTO reaction.

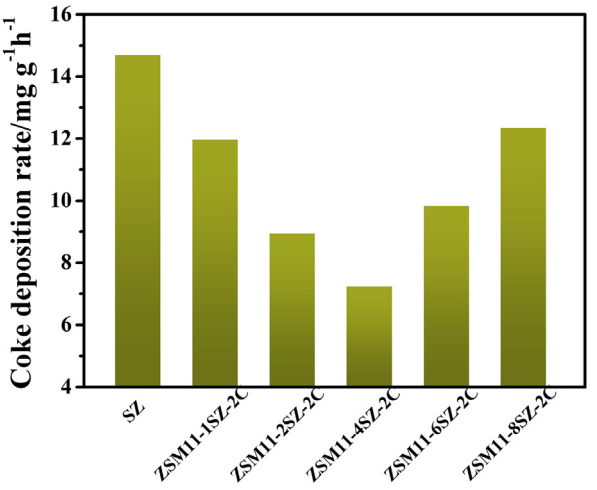

Fig. 8. Carbon deposition rates in the MTO reaction on samples synthesized with different amounts of SZ as seed.

zeolites showed similar propene selectivity and reaction time. Bleken et al. [20] reported that IM-5, TNU-9, ZSM-11, and ZSM-5, with Si/Al = 14–24 and crystal sizes below 2 μm, gave initially full methanol conversion and showed strikingly similar effluent product selectivities. However, their lifetime duration differed significantly, and decreased in the following order: ZSM-11 > ZSM-5 ≥ TNU-9 > IM-5. Meng et al. [18] reported that pure silica zeolite with MEL structure (Si-ZSM-11) was an efficient MTO catalyst, with propene yield of 14 wt % and propene/ethene ratio of 5.9, higher than those over H-ZSM-11 zeolite with a Si/Al ratio of 26, which was attributed to the hydrogen-bonded silanol groups in Si-ZSM-11, which are weakly acidic and act as active sites in methanol conversion that predominantly promote propene production and inhibit side reactions. The catalytic testing was carried out at 723 K. They also studied the methanol to light olefins catalyzed by ZSM-11 with the SiO_2/Al_2O_3 ratio of 65 in a circulating fluidized-bed unit at the temperature of 773 K. The hierarchical ZSM-11 catalyst was highly resistant to coking on the external surface due to the formation of mesopores in the conversion of methanol. ZSM-11 showed better property than ZSM-5 in the formation of light olefins [7]. Conte et al. [19] reported that the intergrowth composite zeolites ZSM-5/11 with a SiO_2/Al_2O_3 ratio of 137 displayed selectivity to propene of up to 50%, and a relative increase over ZSM-5 of ca. 80% under the same reaction conditions.

The high stabilities of the hierarchical ZSM-11/5 composite zeolites can be ascribed to the higher specific surface areas, higher external surface areas, more mesopore volumes, and more acid sites than SZ. With the increase in the amounts of SZ, the specific surface areas, external surface areas, mesopore volumes, and acid sites all increase markedly. On one hand, the larger the specific surface area, the external surface area, and the mesopore volume are, the more acid sites are exposed to the reactants. More acid sites mean slower coverage by deposited carbon. On the other hand, the large mesopore volume can also accommodate more deposited carbon.

With further increase in the amount of SZ in the synthesis to the seed/SiO_2 molar ratio of 6 or above, the catalyst life decreases. At the same time, the proportion of ZSM-5 in the ZSM-11/5 composite zeolite also increases appreciably. ZSM-11 has similar pore size as ZSM-5. However, ZSM-5 has intersecting straight and sinusoidal channels, whereas ZSM-11 has intersecting straight channels, and therefore bigger intersection spaces. It is conceivable that the bigger intersection spaces of ZSM-11 can also accommodate more deposited carbon than ZSM-5. Therefore, with the addition of too much of SZ, the catalyst life decreases because the proportion of ZSM-5 in the ZSM-11/5 composite zeolite increases appreciably. Interestingly, it was reported that ZSM-11 can also catalyze ethanol to propene reaction with high selectivity [9,23]. Liu et al. [23] found that compared to ZSM-5 with the same SiO_2/Al_2O_3 ratio, ZSM-11 possesses higher stability, which was also ascribed to the larger size of the intersections.

4. Conclusions

Hierarchical ZSM-11/5 composite zeolite with a high SiO_2/Al_2O_3 ratio was successfully synthesized using a seed-induced method in the presence of CTAB. The amount of seed added plays a key role in the formation of the ZSM-11/5 composite with hierarchical pores. With the increase in the amount of seed, the composite zeolites exhibits larger specific surface areas, larger external surface areas, larger mesopore volumes, and more acid sites than ZSM-11 synthesized by the conventional method with tetrabutylammonium ions as template and show excellent catalytic properties in the reaction of MTOs.

Contrary to the conventional point of view, addition of too much seeds results in the formation of the ZSM-11/5 composite zeolite with a high proportion of ZSM-5. Although the composite zeolite still has a large specific surface area, a large external surface area, a large mesopore volume, and a large number of acid sites, the catalytic performance decreases drastically.

Acknowledgments

This work has been supported by the National Natural Science Foundation of China (grant no. 21276183).

References

[1] P. Chu, N.J. Woodbury, US Patent 3,709,979, 1973.
[2] G.T. Kokotailo, P. Chu, S.L. Lawton, W.M. Meier, Nature 275 (1978) 119.
[3] A.M. Varvarin, K.M. Khomenko, V.V. Brei, Fuel 106 (2013) 617.
[4] M.S. Renzini, U. Sedran, L.B. Pierella, J. Anal. Appl. Pyrolysis 86 (2009) 215.
[5] S. Follmann, S. Ernst, New J. Chem. 40 (2016) 4414.
[6] M. Dyballa, P. Becker, D. Trefz, E. Klemm, A. Fischer, H. Jakob, M. Hunger, Appl. Catal. A 510 (2016) 233.
[7] X.J. Meng, H.W. Huang, Q. Zhang, M.X. Zhang, C.Y. Li, Q.K. Cui, Korean J. Chem. Eng. 33 (2016) 831.
[8] H.W. Huang, X.J. Meng, C. Chen, M.X. Zhang, Z. Meng, C.Y. Li, Q.K. Cui, Catal. Lett. 146 (2016) 2357.
[9] K. Inoue, K. Okabe, M. Inaba, I. Takahara, K. Murata, React. Kinet. Mech. Cat. 101 (2010) 227.
[10] X.J. Meng, C. Chen, J.W. Liu, Q. Zhang, C.Y. Li, Q.K. Cui, Appl. Petrochem. Res. 6 (2016) 41.

[11] L.C. Lerici, M.S. Renzini, U. Sedran, L.B. Pierella, Energy Fuels 27 (2013) 2202.
[12] O.A. Anunziata, G.V.G. Mercado, L.B. Pierella, Catal. Lett. 87 (2003) 167.
[13] O.A. Anunziata, G.A. Eimer, L.B. Pierella, Catal. Lett. 58 (1999) 235.
[14] O.A. Anunziata, G.V.G. Mercado, L.B. Pierella, Catal. Lett. 75 (2001) 93.
[15] T.L.M. Maesen, M. Schenk, T. Vlugt, B. Smit, J. Catal. 203 (2001) 281.
[16] Y. Gu, N. Cui, Q. Yu, C. Li, Q. Cui, Appl. Catal. A 429 (2012) 9.
[17] Q. Yu, C. Cui, Q. Zhang, J. Chen, Y. Li, J. Sun, C. Li, Q. Cui, C. Yang, H. Shan, J. Energy Chem. 22 (2013) 761.
[18] X. Meng, Q. Yu, Y. Gao, Q. Zhang, C. Li, Q. Cui, Catal. Commun. 61 (2015) 67.
[19] M. Conte, B. Xu, T.E. Davies, J.K. Bartley, A.F. Carley, S.H. Taylor, K. Khalid, G.J. Hutchings, Microporous Mesoporous Mater. 164 (2012) 207.
[20] F. Bleken, W. Skistad, K. Barbera, M. Kustova, S. Bordiga, P. Beato, K.P. Lillerud, S. Svelle, U. Olsbye, Phys. Chem. Chem. Phys. 13 (2011) 2539.
[21] L. Zhang, H.J. Liu, X.J. Li, S.J. Xie, Y.Z. Wang, W.J. Xin, S.L. Liu, L.Y. Xu, Fuel Process. Technol. 91 (2010) 449.
[22] X.J. Li, C.F. Wang, S.L. Liu, W.J. Xin, Y.Z. Wang, S.J. Xie, L.Y. Xu, J. Mol. Catal. A: Chem. 336 (2011) 34.
[23] D.P. Liu, Y. Liu, E.Y.L. Goh, C.J.Y. Chu, C.G. Gwie, J. Chang, A. Borgna, Appl. Catal. A 523 (2016) 118.
[24] S. Mintova, N. Petkov, K. Karaghiosoff, T. Bein, Microporous Mesoporous Mater. 50 (2001) 121.
[25] G.R. Millward, S. Ramdas, J.M. Thoma, J. Chem. Soc. Faraday Trans. 79 (1983) 1075.
[26] G.A. Jablonski, L.B. Sand, Zeolites 6 (1986) 396.
[27] C.A. Fyfe, Z.S. Lin, C. Tong, R.J. Darton, Microporous Mesoporous Mater. 150 (2012) 7.
[28] P.F. Xie, Y.J. Luo, Z. Ma, C.Y. Huang, C.X. Miao, Y.H. Yue, W.M. Hua, Z. Gao, J. Catal. 330 (2015) 311.
[29] H. Liu, S.J. Xie, W.J. Xin, S.L. Liu, L.Y. Xu, Catal. Sci. Technol. 6 (2016) 1328.
[30] Q.J. Yu, C.Y. Li, X.L. Tang, H.H. Yi, J. Porous. Mater. 23 (2016) 273.
[31] Q.J. Yu, J. Chen, Q. Zhang, C.J. Li, Q.K. Cui, Mater. Lett. 120 (2014) 97.
[32] X.W. Guo, Y.H. Liu, X.S. Wang, Y.Y. Chen, W.P. Zhang, X.W. Han, X.H. Bao, L.W. Lin, J. Dalian, Univ. Technol. 41 (2001) 426.
[33] K.P. Dey, S. Ghosh, M.K. Naskar, Mater. Lett. 87 (2012) 87.
[34] D. Uzcátegui, G. González, Catal. Today 107 (2005) 901.
[35] H.L. Chen, J. Ding, Y.M. Wang, New J. Chem. 38 (2014) 308.
[36] Q.J. Yu, C.Y. Li, X.L. Tang, H.H. Yi, Ind. Eng. Chem. Res. 54 (2015) 2120.
[37] K. Ozawa, R. Okada, Y. Nakao, T. Ogiwara, H. Itoh, F. Iso, J. Am. Ceram. Soc. 93 (2010) 4022.
[38] J. Dong, J. Zou, Y. Long, Microporous Mesopoous. Mater. 57 (2003) 9.
[39] G. Gonzalez, M.E. Gomes, G. Vitale, G.R. Castro, Microporous Mesoporous Mater. 121 (2009) 26.
[40] X. Zhang, D. Liu, D. Xu, S. Asahina, K.A. Cychosz, K.V. Agrawal, Y.A. Wahedi, A. Bhan, S.A. Hashimi, O. Terasaki, M. Thommes, M. Tsapatsis, Science 336 (2012) 1684.
[41] D. Xu, G.R. Swindlehurst, H. Wu, D.H. Olson, X. Zhang, M. Tsapatsis, Adv. Funct. Mater. 24 (2014) 201.
[42] H.B. Zhu, Z.C. Liu, D.J. Kong, Y.D. Wang, Z.K. Xie, J. Phys. Chem. C 112 (2008) 17257.
[43] M.Y. Kustova, P. Hasselriis, C.H. Christensen, Catal. Lett. 96 (2004) 205.
[44] K. Egeblad, M. Kustova, S.K. Klitgaard, K. Zhu, C.H. Christensen, Microporous Mesoporous Mater. 101 (2007) 214.
[45] Q.J. Yu, X.L. Tang, H.H. Yi, Chem. Eng. J. 314 (2017) 212.
[46] J.O. Abildstrøm, Z.N. Ali, U.V. Mentzel, J. Mielby, S. Kegnæs, M. Kegnæs, New J. Chem. 40 (2016) 4223.
[47] W.S. Zhang, S. Zhang, W.J. Xin, H. Liu, Y.C. Shang, X.X. Zhu, S.L. Liu, L.Y. Xu, J. Energy Chem. 26 (2017) 380.
[48] Q.J. Yu, X.L. Tang, H.H. Yi, Mater. Chem. Phys. 202 (2017) 377, https://doi.org/10.1016/j.matchemphys.2016.12.004.
[49] Y. Nakagawa, WO Patent 9,509,812, 1995.
[50] Y. Nakagawa, G.S. Lee, T.V. Harris, L.T. Yuen, S.I. Zones, Microporous Mesoporous Mater. 22 (1998) 69.
[51] P.M. Piccione, M.E. Davis, Microporous Mesoporous Mater. 49 (2001) 163.
[52] R. Marguta, S.J. Khatib, J.M. Guil, E. Lomba, E.G. Noya, J.A. Perdigón-Melón, S. Valencia, Microporous Mesoporous Mater. 142 (2011) 258.
[53] Y.S. Tao, H. Kanoh, L. Abrams, K. Kaneko, Chem. Rev. 106 (2006) 896.
[54] W. Song, Z.T. Liu, L.P. Liu, A.L. Skov, N. Song, G. Xiong, K.K. Zhu, X.G. Zhou, RSC Adv. 5 (2015) 31195.
[55] L. Chen, S.Y. Zhu, Y.M. Wang, M.Y. He, New J. Chem. 34 (2010) 2328.
[56] Q.J. Yu, C.Y. Li, X.L. Tang, H.H. Yi, RSC Adv. 5 (2015) 8152.
[57] H. Liu, S.L. Liu, S.J. Xie, C. Song, W.J. Xin, L.Y. Xu, Catal. Lett. 145 (2015) 1972.
[58] B. Xie, J. Song, L. Ren, Y. Ji, J. Li, F.-S. Xiao, Chem. Mater. 20 (14) (2008) 4535.
[59] Q.J. Yu, X.J. Meng, J.W. Liu, C.Y. Li, Q.K. Cui, Microporous Mesoporous Mater. 181 (2013) 192.
[60] X. Wang, H.B. Chen, F.J. Meng, F. Gao, C. Sun, L.Y. Sun, S.H. Wang, L. Wang, Y.Q. Wang, Microporous Mesoporous Mater. 243 (2017) 271.
[61] J. Ahmadpour, M. Taghizadeh, C. R. Chimie 18 (2015) 834.
[62] P. Losch, M. Boltz, B. Louis, S. Chavan, U. Olsbye, C. R. Chimie 18 (2015) 330.
[63] R.N.M. Missengue, P. Losch, G. Sedres, N.M. Musyoka, O.O. Fatoba, B. Louis, P. Pale, L.F. Petrik, C. R. Chimie 20 (2017) 78.
[64] H.B. Chen, Y.Q. Wang, F.J. Meng, H.Y. Li, S.G. Wang, C. Sun, S.H. Wang, X. Wang, Microporous Mesoporous Mater. 244 (2017) 301.
[65] F.J. Meng, Y.Q. Wang, S.G. Wang, X. Wang, S.H. Wang, C. R. Chimie 20 (2017) 385.
[66] H.B. Chen, Y.Q. Wang, F.J. Meng, H.Y. Li, S.G. Wang, C. Sun, S.H. Wang, X. Wang, RSC Adv. 80 (2016) 76642.
[67] X.F. Yu, L.Y. Zhao, X.X. Gao, X.P. Zhang, N.Z. Wu, J. Solid State Chem. 179 (2006) 1525.
[68] J. Garcia-Martinez, C.H. Xiao, K.A. Cychosz, K.H. Li, W. Wan, X.D. Zou, M. Thommes, ChemCatChem 6 (2014) 3110.
[69] J. Garcia-Martinez, M. Johnson, J. Valla, K. Li, J.Y. Ying, Catal. Sci. Technol. 2 (2012) 987.
[70] V. Blay, B. Louis, R. Miravalles, T. Yokoi, K.A. Peccatiello, M. Clough, B. Yilma, ACS Catal. 7 (2017) 6542.